

SHELL STRUCTURE OF TEREBRATULID BRACHIOPODS

by D. I. MACKINNON and A. WILLIAMS

ABSTRACT. Ultrastructural studies of living and fossil brachiopods belonging to the Terebratulidae show that the shell is invariably penetrated by unbranched puncta and generally consists of a three-fold mineral succession: a primary layer composed of acicular and granular crystallites, a secondary layer of orthodoxy stacked fibres, and a prismatic tertiary layer. The constituents of the last layer are not 'prisms' in the crystallographic sense but discrete units with interlocking boundaries arranged normal to the surface of accretion. Each prism arises from a fibre first by lateral spreading of the terminal face and then by vertical accretion so that growth banding no longer indicates an oblique increase in length as in fibres. Sections of decalcified mantle show that the epithelium secreting the tertiary layer is like that underlying the secondary shell except that it does not exude proteinous sheets between prisms. Amalgamation of prisms may, therefore, be inhibited by either sheets of water-soluble organic compounds or crystallographic incompatibility between adjacent prisms as indicated by non-alignment of cleavage. The tertiary layer was not developed in *Lobothyris*, the oldest terebratulid studied, so that the layer was possibly first acquired gerontomorphically. But it is also lacking in the shell of other genera like *Rhombothyris* and *Terebratula* and this may reflect repeated neotenuous suppression. Despite the uniform texture of the tertiary layer, expansion of muscle bases across overlying epithelium causes different types of myotests to develop in *Liothyrella* and *Gryphus* as in other living articulate. The characteristic well-ordered pits in *Liothyrella*, in particular, suggest that the disposition and strength of muscle fibres contribute to the shaping of myotest topography.

THE three-fold skeletal succession characteristic of most living articulate brachiopods was first recognized by King in 1871. Carpenter had previously identified an external organic cover, named the periostracum by him, and an underlying calcareous layer which he described (1853, pp. 25–26) as consisting exclusively of 'flattened prisms, of considerable length, arranged parallel to each other with great regularity and at a very acute angle—usually only about 10° or 12° —with the surface of the shell'. In fact an equally distinctive thin compact layer of cryptocrystalline calcite, referred to as the laminar layer by its discoverer King (1871, p. 441), intervenes between the periostracum and the very much thicker succession of so-called calcite prisms. The 'laminar' and 'prismatic' layers are now distinguished as 'primary' and 'secondary' respectively (Williams 1956, p. 246; 1968, p. 2) to indicate their relative order of deposition within the standard secretory regime of articulate brachiopods. Indeed the terms laminar and prismatic are even inappropriate as descriptions of the dominant fabric of each layer. The primary layer consists of crystallites usually aligned normal to the external surface, and any growth banding developed does not form discrete laminae. Similarly, the calcite components of the secondary shell are not prisms in the crystallographic sense but fibres sheathed in interconnected proteinous membranes and tightly stacked in regular alternating rows. Hobbs and Cloud (in Cloud 1942, p. 24) have shown that the optical c-axis of calcite in crushed fragments of the secondary shell makes an angle of about 25° with the long axis of constituent fibres. This arrangement is consistent with a c-axis orientation more or less normal to the terminal growth face of a fibre and, therefore, to any growth banding seen in sagittal sections of fibres. In addition to the finely crystalline and fibrous textures of the carbonate shell successions of non-strophomenide articulates, a third fabric is

fairly commonly developed. So far as we are aware, it was first explicitly identified as being characteristic of a third layer succeeding the 'inner and outer shell layers' by Alexander (1948, p. 48) in her study of Silurian pentameraceans. Like many others authors including St. Joseph (1938, p. 241) and Amsden (1964, p. 222), Alexander referred to this fabric as prismatic, presumably because the mineral constituents are 'prisms having their long axes perpendicular to the shell surface' (Gauri and Boucot 1968, p. 87). In this context 'prismatic' is the most appropriate term available to describe the texture of the layer although few of the lateral walls of crystallites are demonstrably $\{10\bar{1}0\}$ faces.

Prismatic shell is widely distributed among extinct brachiopods being especially characteristic of pentamerides and spiriferides. In skeletal successions of species belonging to these two orders, prisms may have developed as impersistent lenses as well as a distinct tertiary layer. Under the optical microscope the fibrous and prismatic layers are seen to pass into one another without the intervention of any sharply defined interface (Williams and Rowell in Williams *et al.* 1965, p. H64). But the nature of the passage remained tantalizingly obscure until one of us (MacKinnon 1971) observed under the scanning electron microscope the exact relationship between fibres and prisms in the shells of the Triassic spiriferide *Koninckina leonhardi* (Wissman) and the living terebratulide *Gryphus vitreus* (Born). The occurrence of a prismatic tertiary layer in the latter genus which was first reported by Sass and Munroe (1967, p. 302), was especially significant because it indicated that it would be possible to determine the type of outer epithelium responsible for the secretion of prismatic calcite. The specimens of *Gryphus* used in that investigation had been preserved in alcohol for more than 50 years and sections of decalcified shell and mantle were not well enough preserved for study under a transmission electron microscope. Fortunately, however, the more easily obtainable related species, *Liothyrella neozelanica* Thomson, also proved to have a prismatic layer in its shell, and living specimens have been successfully prepared for the study of tissue ultrastructure.

Finally, although this paper is not intended to be a comprehensive survey of prismatic calcite occurring in the shell of articulate brachiopods, we thought it appropriate to ascertain whether it is found in other Terebratulidae. It is not anticipated, however, that the development of prismatic shell among terebratulides is restricted to members of that family especially when one considers the size and thickness of many centronellidine shells.

Materials and Methods. Specimens used in the researches described below were obtained in the living, dried, or fossilized state and have been variously treated in the following manner. For study of the mantle under the transmission electron microscope, living specimens were fixed in 4% glutaraldehyde made up in 3% sodium chloride, then decalcified in 10% EDTA, washed in sucrose, and treated for 1 hour with 2% osmic acid; all solutions were buffered to pH 7.2 with phosphate buffer. Following dehydration, specimens were embedded in an Epoxy resin and the microtomed sections were stained with aqueous uranyl acetate and aqueous lead citrate. All shells of living and fossil species were studied under a Stereoscan electron microscope (NERC grant GR/3/443). For this purpose the valves of living and dried specimens were freed of soft parts by immersion in sodium hypochlorite for some hours. Next, any loosely adherent particles were removed from natural and fracture surfaces by brief sonication in a weak detergent and then in acetone. Many fossils examined were embedded in rock matrix and details of their skeletal successions are best seen in cut sections. Consequently, Recent shells have also been sectioned in the same way to ensure that details of fossil successions have been correctly identified. For this purpose, both fossils in matrix and free shells were embedded in a resin, like Araldite, and cut with a diamond-edged blade along any preferred direction

to provide surfaces containing the required sections. These were then polished with tin oxide or alumina and etched in 2% EDTA for up to 30 minutes, dependent on the texture and geological age of the shell, to accentuate topographic differences between various microscopic features. All natural surfaces, fracture surfaces, and differentially etched sections were coated with gold/palladium for examination under the Stereoscan.

STRUCTURE OF *LIOTHYRELLA* SHELL

Mantle and caeca. The mantle of *Liothyrella neozelanica* Thomson, with its densely distributed microscopic cylindroid outgrowths (caeca) accommodated by canals (puncta) permeating the calcareous shell and its meshwork of spicules, is essentially like that of the terebratulacean *Terebratulina retusa* (Linnaeus) (Williams 1968, p. 279). The mantle edge was not preserved in its entirety in the sections examined because decalcification caused the periostracum, which has not been seen, to pull away from, and rupture, the outer mantle lobe. However, enough of the outer mantle lobe survives to show that it is composed of elongate secretory cells, with large nuclei and many secretion droplets in various stages of depletion, representing immature outer epithelium. These cells are separated from the ciliated and microvillous inner epithelium by a narrow generative zone, more or less coinciding with the closure of the mantle groove, from which both kinds of epithelia are proliferated. Thus as each newly generated cell rotates around the outer mantle lobe to become part of the outer epithelium lining a valve, it successively secretes periostracum, primary crystallites, secondary fibres, and tertiary prisms. This sequence represents the secretory regime of *Liothyrella*. Consequently, any differences between epithelial cells associated with the various carbonate layers at the moment of death may be regarded as indicating the kind of changes each cell undergoes as it becomes increasingly distant from the radially expanding mantle edge.

The unbranched caeca of *Liothyrella* are similar to those found in *Waltonia inconspicua* (Sowerby) and evidently originate in the same way by differentiation of groups of migrating cells at the mantle edge (Owen and Williams 1969). The core cells are well developed as pendent clusters surrounded by flattened peripheral cells which form the caecal wall and are continuous basally with the outer epithelium of the mantle. The core cells are storage centres being charged with lipids and glycogen rosettes and especially spheroidal membrane-bound secretion droplets of protein up to 1 μm in diameter and much larger ellipsoidal electron-light bodies of mucoprotein without confining membranes (Pl. 21, fig. 2). The distal plasmalemmas of the core cells are prolonged into microvilli, up to 180 nm in diameter, which are small enough to have filled a series of canals penetrating a canopy of primary calcite, about 4 μm thick, between the caecum and the periostracum. The canopy canals are lined with the same electron-dense proteinous membrane, about 7 nm thick, separating the peripheral flattened cells of a caecum from the walls of its punctum. Within the canals the membrane forms polysaccharide-filled prolongations (the brush) (Pl. 21, fig. 1). Elsewhere the membrane, which is attached to peripheral cells by numerous desmosomes, probably inhibits further carbonate deposition within the punctum (Pl. 21, fig. 3). Caeca are accommodated by puncta about 10 μm in diameter proximally but widening to about 15 μm towards the distal termination. Since they normally remain functional throughout the life of the animal, they provide reliable checks on the extent of various shell layers in decalcified sections.

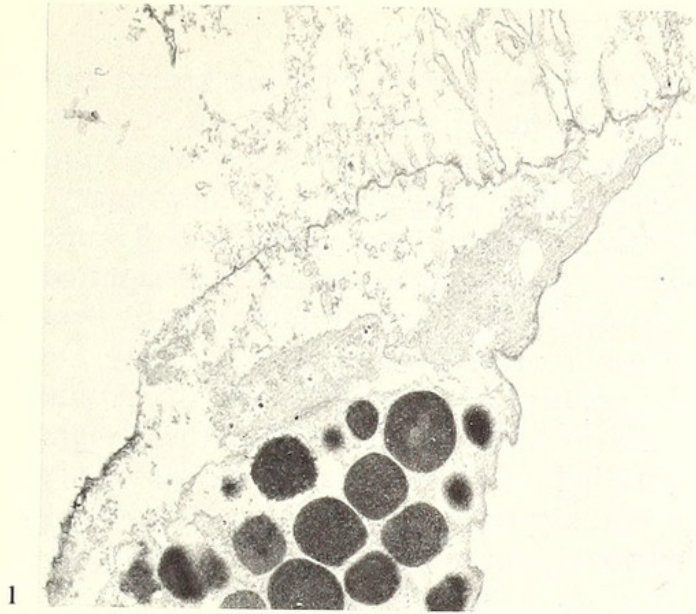
Primary and secondary layers. Cells secreting the primary layer are horizontally elongate and highly vesicular with much glycogen in the groundmass and glycoprotein residues in the secretion droplets (Pl. 21, fig. 4). Secretory plasmalemmas are less coarsely microvillous than those responsible for the exudation of the periostracum. Another distinctive feature of these cells is the presence of a discontinuous layer of electron-dense particles, no more than a few nanometres in size, disposed at about 10 nm external to the plasmalemmas. The primary layer is only about 30 μm thick and forms a rim at the edge of each valve up to 30 μm wide (Pl. 22, fig. 4). Judging from the occurrence of fine banding with a periodicity of about 250 nm, the growth surfaces, on which the outer epithelial cells rest (the superficial synchronous boundary), are inclined at about 25° to the isotopic secondary junction (Pl. 23, fig. 1). The layer is composed of solidly compacted acicular crystallites about 1 μm wide and up to 15 μm long arranged more or less normal to the growth surface. These crystallites impart a granular texture to the growth surface except where groups of them amalgamate to form cleaved nodules 3 μm or more in size (Pl. 22, fig. 5).

Inwardly towards the primary-secondary junction the epithelial cells change in structure and topography as they begin simultaneously to secrete protein as well as calcite and to accommodate arrays of secondary fibres. The cells become flattened so that they do not stand much more than a micron above the basal lamina except between fibres where narrow zones may extend into the secondary shell for 2 or more microns (Pl. 21, fig. 5). The chief internal differences include: more numerous mitochondria, a reappearance of abundant glycoprotein droplets, a tendency for vesicles to become fewer but large, and especially the development of tonofibrils. The tonofibrils normally extend from the basal lamina to the secretory plasmalemma. They are densely distributed in the inter-fibre zones where they pass into desmosomes connecting the plasmalemma to an external proteinous sheet about 20 nm distant. Each proteinous sheet, which is a triple-unit membrane about 7 nm thick, is continuous with those secreted by adjacent cells. They are, therefore, secreted as complete wrappings to fibres except on the terminal faces of fibres where the plasmalemma is filamentous but otherwise free of an external organic coat.

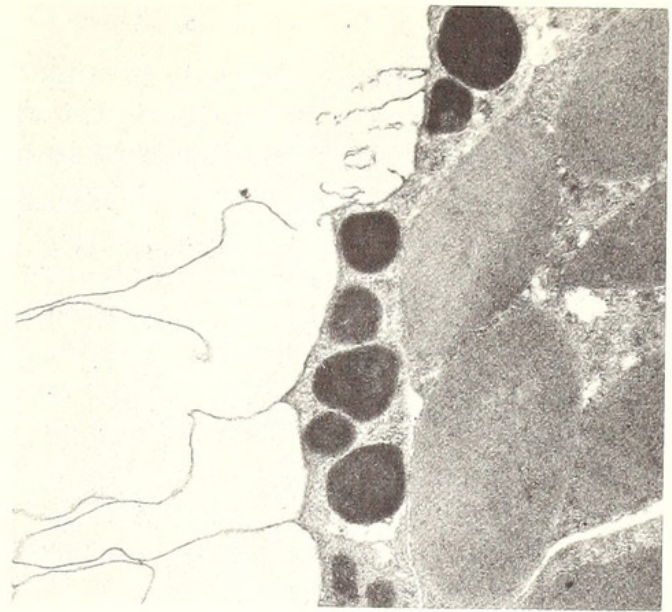
The fibres are essentially like those found in the secondary shell of most articulate

EXPLANATION OF PLATE 21

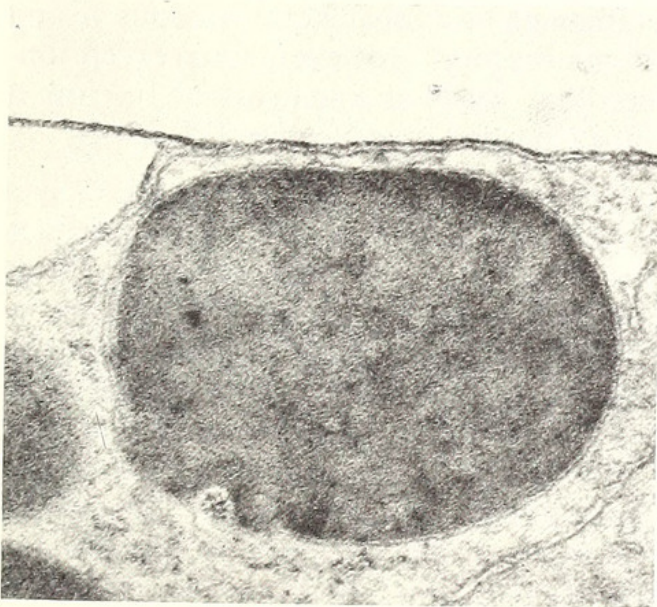
Figs. 1–5. Transmission electron micrographs of decalcified shell and mantle of *Liothyrella neozelanica* Thomson; Recent, Farewell Spit, S. Island, New Zealand. 1. Lateral longitudinal section through the distal part of a caecum showing the brush towards the top and flattened peripheral cells with conspicuous proteinous secretion droplets below ($\times 5150$). 2. Sagittal section through a caecum at the junction of the primary and secondary carbonate layers indicated respectively by the absence (top left) or presence (bottom left) of interconnected proteinous sheets; flattened peripheral cells containing proteinous droplets occur in the middle and core cells filled with elliptical mucoproteinous inclusions to the right ($\times 8200$). 3. Sagittal section of part of a flattened peripheral cell showing the desmosomal connections between continuous proteinous sheets and the plasmalemma ($\times 68750$). 4. Section of part of an outer epithelial cell responsible for the secretion of the primary shell showing the discontinuous proteinous sheet associated with the plasmalemma; connective tissue with collagens (below) separated from the outer epithelium by a basal lamina ($\times 55000$). 5. Oblique section through the outer epithelium responsible for the secretion of the secondary shell showing interconnected proteinous sheets and their desmosomal attachments to external plasmalemmas ($\times 17200$).



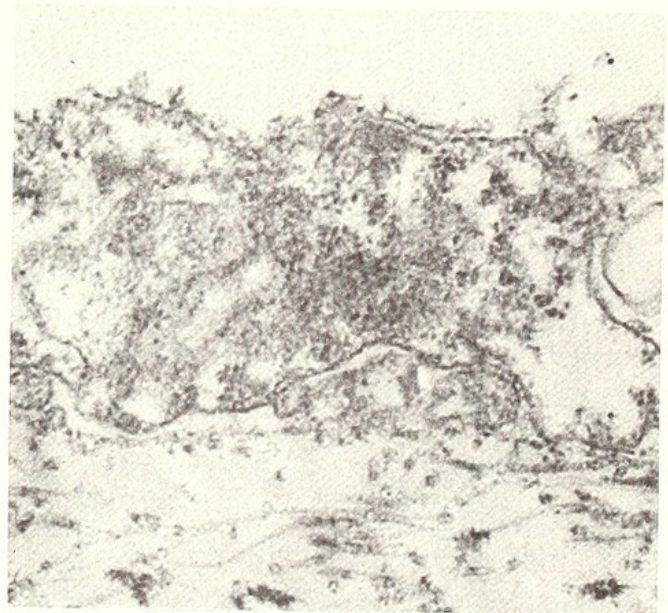
1



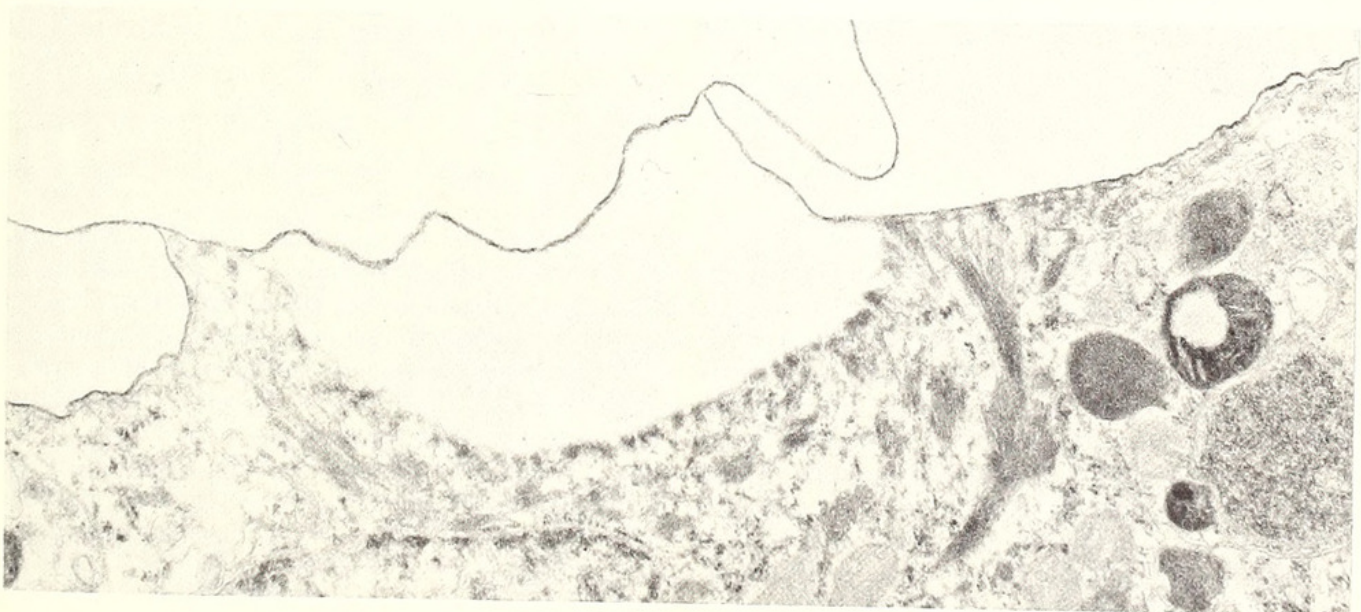
2



3



4



5

brachiopods, being regularly arranged in alternating rows and having keeled and convex outer and inner surfaces respectively (Pl. 23, fig. 4). There are, however, noteworthy differences. The first-formed fibres, which are usually no more than 4 μm wide, may form loosely packed aggregates disposed at a high angle to the primary-secondary junction (Pl. 22, figs. 4, 5). Their terminal faces, as well as those of some mature fibres which are normally over twice as big, may have truncated or squared rather than rounded outer boundaries (Pl. 23, fig. 2). All types of fibres usually bear traces of variation in calcite secretion which may represent a diurnal periodicity. On fibre surfaces, these traces consist of ridges arranged at intervals of about 300 nm parallel with the rhombic corner angles of orthodox terminal faces or with the straight outer boundaries of the square-ended ones (Pl. 23, fig. 3). In sections of the secondary layer such variation in carbonate secretion is indicated by curved growth banding disposed more or less normal and tangential to the outer and inner surfaces respectively of fibres.

In contrast to the relatively coarse texture of the primary shell, the fibres of the secondary shell are generally so finely crystalline as to appear homogeneous within the resolution limits of the scanning electron microscope. However, some exceptionally well-preserved terminal faces bear 'spheroidal' seeds of calcite about 100 nm in size and these appear to be the basic units in carbonate precipitation (Pl. 23, fig. 3).

Tertiary layer. The passage from secondary fibres to fully developed prismatic calcite is less abrupt than the change from primary to secondary shell. On the internal surface of adult valves, secondary fibres occupy a band about 1.5 mm wide. But many fibres within the innermost third of that band exhibit some of the characteristic features of the prismatic layer, the extent of which has been conveniently determined as the area in which no recognizable fibres survive. This transitional zone coincides in section with the occurrence of impersistent lenses of prismatic calcite interfingering with regularly arranged fibres (Pl. 24, fig. 3) representing slight transgressions and regressions of the secondary-tertiary boundary during shell deposition. The change in the secretory regime of the outer epithelium, on the other hand, is immediately indicated by cessation in protein exudation. In decalcified sections this change is represented by the abrupt termination along a fairly constant horizon of the protein sheets ensheathing secondary fibres (Pl. 22, fig. 1). Consequently cells separated by

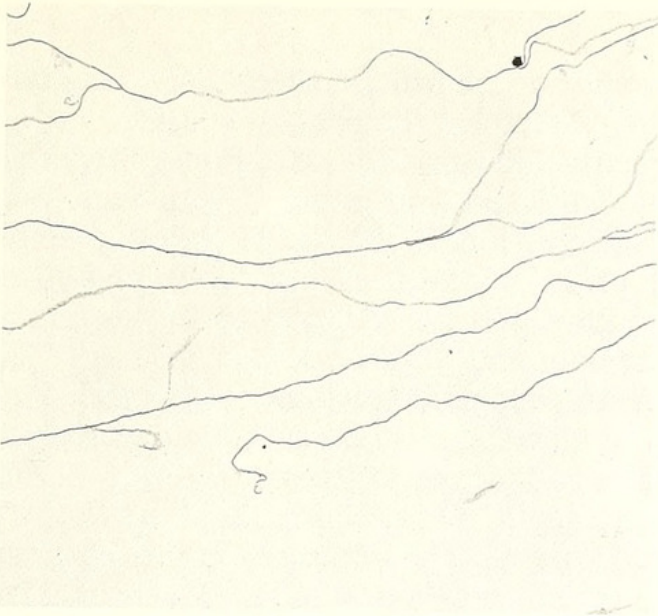
EXPLANATION OF PLATE 22

Figs. 1-3. Transmission electron micrographs of decalcified shell and mantle of *Liothyrella neozelanica*.

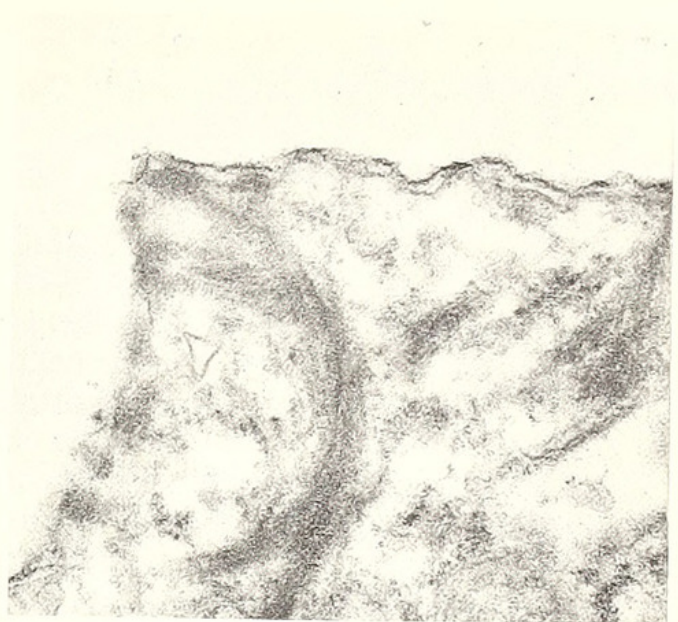
1. Section showing terminations of interconnected proteinous sheets pervading the secondary layer at its junction with the tertiary layer (below) ($\times 14000$). 2. Section through part of an outer epithelial cell responsible for the secretion of the tertiary shell showing continuous proteinous sheets connected by desmosomes to the plasmalemma ($\times 55000$). 3. Oblique section through the outer epithelium underlying the tertiary layer showing the absence of proteinous sheets within the layer (above); connective tissue with collagens (below) separated from the outer epithelium by a basal lamina ($\times 8200$).

Figs. 4-5. Scanning electron micrographs of the shell of *Liothyrella neozelanica*. 4. Internal surface of the antero-medial edge of the brachial valve showing the primary and secondary layers with puncta ($\times 1300$). 5. Detail of internal surface of the antero-medial edge of the brachial valve showing the junction between the primary layer (below) and the first-formed secondary fibres (above) ($\times 6700$).

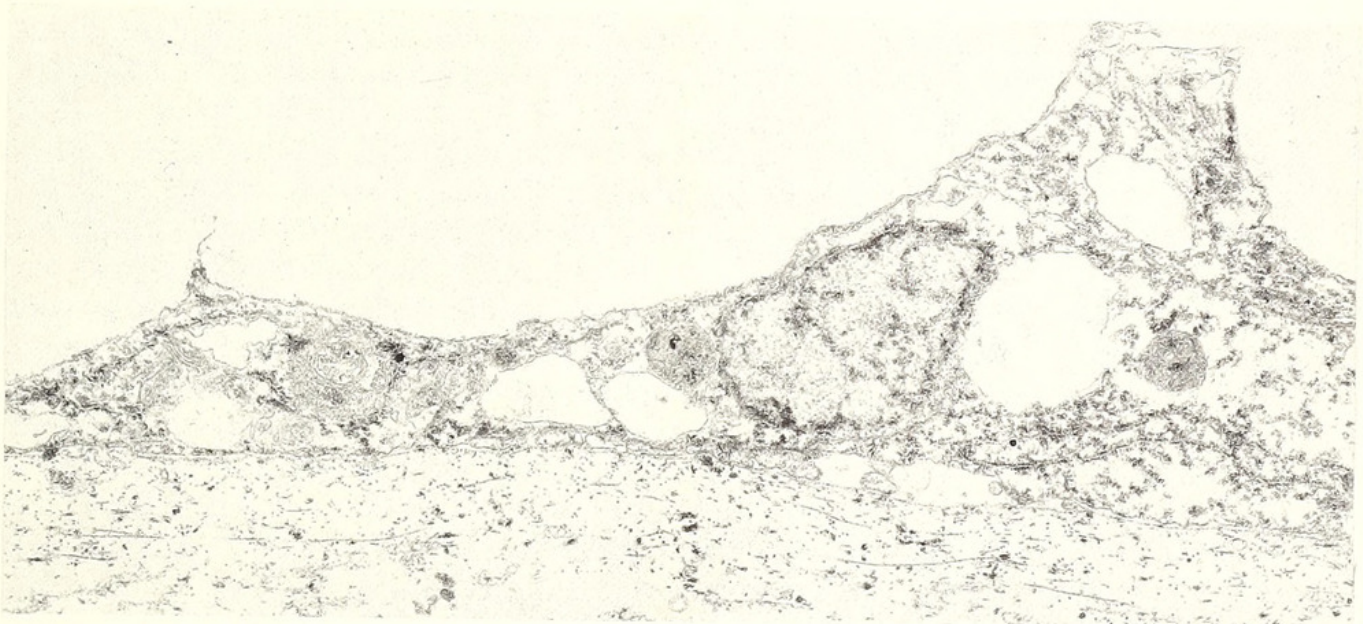
1



2



3



4



5



MACKINNON and WILLIAMS, terebratulid shell

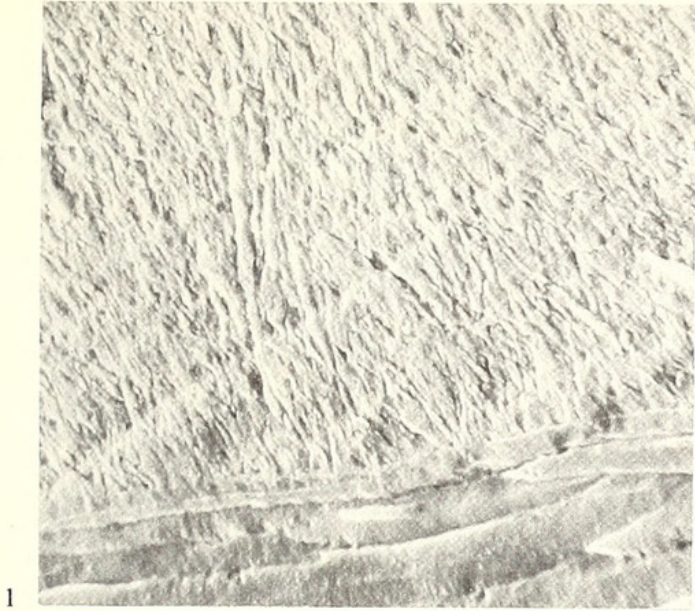
a space of variable thickness from the free ends of the protein sheets pervading the secondary shell, are identifiable as those which secreted the prismatic layer.

Cells secreting prismatic calcite do not greatly differ from those responsible for the deposition of secondary fibres, being also flattened and charged with secretion droplets of glycoproteins in various stages of depletion (Pl. 22, fig. 3). Indeed despite the absence of organic membranes in the prismatic layer, even a continuous proteinous sheet, up to 10 nm thick, persists about 20 nm external to the secreting plasmalemma to which it is attached by septate and fibrillar desmosomes (Pl. 22, fig. 2). This monolayer, like its counterparts in younger epithelium, is interpreted as the outer boundary to a film of extracellular fluid which sustains carbonate secretion.

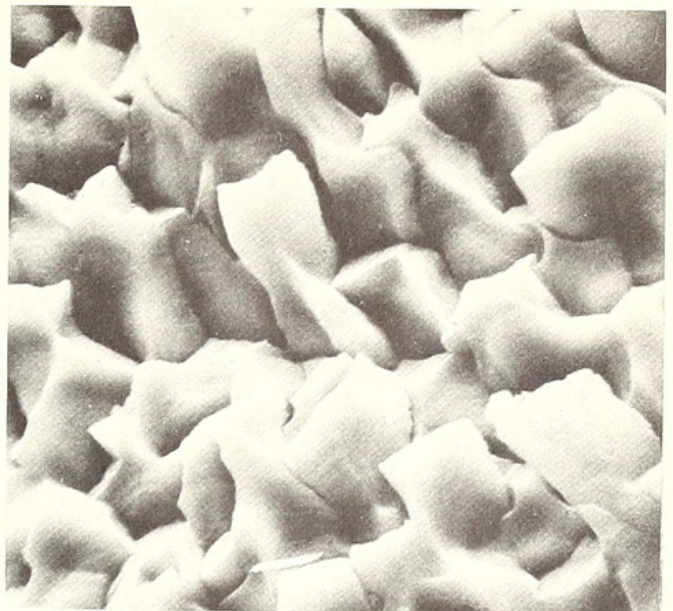
The first sign of the change in carbonate secretion, which ultimately results in the deposition of a continuous layer of prismatic calcite, is the occurrence of malformed fibres on the internal surface of a valve (Pl. 23, fig. 5). The irregular outlines of these fibres are due to the differential lateral growth and resorption of the distal edges of their terminal faces. Continued lateral expansion causes these crenulated edges to interlock into a coarsely granular mosaic covering the regularly arranged fibres. Organic secretion must cease at this stage in the deposition of the prismatic layer. The stage is represented in section by a sudden swelling of the fibres into prisms three or four times as thick, and a concomitant reorientation of the carbonate constituents to lie normal rather than oblique to the plane of the outer epithelium (Pl. 24, fig. 2). On the surface of this mosaic, too, there is evidence that cells no longer correspond with prisms on a one-to-one ratio as they do with fibres. Sets of arcuate grooves and ridges about 400 nm apart and about 25 μm from another series subtending a rhombic angle commonly occur straddling the boundaries of adjacent prisms (Pl. 23, fig. 6). Such complementary sets of impressions are like the outlines of the terminal faces of fibres and are believed to represent the distal and proximal boundaries respectively of an outer epithelial cell. A noteworthy feature of the prismatic layer, even in these early stages of accretion is the way most extensions of the fibres, irrespective of size or persistence, remain discrete units. Since there are no enveloping proteinous sheets present to prevent lateral intergrowth as in secondary fibres, it is likely that either a water-soluble organic material occupies the interprismatic spaces *in vivo* and is lost in the preparation of sections, or the general lack of epitaxial alignment in adjacent 'prisms' precludes their amalgamation.

EXPLANATION OF PLATE 23

Figs. 1–6. Scanning electron micrographs of the internal surface and sections of a brachial valve of *Liothyrella neozelanica*. 1. Submedial longitudinal section of the primary layer showing the acicular crystallites and growth bands disposed at acute angles to the primary–secondary junction below ($\times 2700$). 2. Internal surface of secondary layer showing fibres with truncated edges to terminal faces ($\times 2600$). 3. Internal surface of secondary layer showing fibres with rounded edges to terminal faces and growth banding ($\times 2000$). 4. Transverse section of the secondary layer showing the characteristic outline and stacking of fibres; infilled punctum on right ($\times 2400$). 5. Internal surface showing the transitional area between the secondary and tertiary layers characterized by malformed fibres ($\times 2600$). 6. Internal surface showing the transitional area between the secondary and tertiary layers with outlines of epithelial cells impressed as grooves and ridges on a mosaic of expanded terminal faces ($\times 2600$).



1



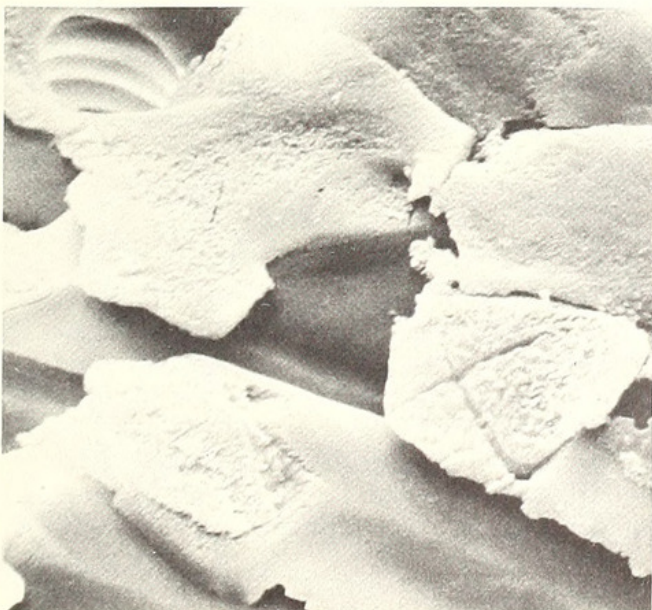
2



3



4



5



6

MACKINNON and WILLIAMS, terebratulid shell

Once secretion of prismatic shell has begun, it may continue and give rise to an ever-thickening layer, or it may be temporarily interrupted by reversion to secondary shell secretion. The latter phase is represented in sections of a valve by isolated lenses of prismatic calcite within a succession of fibres or as wedge-like sheets of the tertiary layer tapering peripherally to interfinger with the secondary layer (Pl. 24, fig. 3). Such sheets and lenses may be more than 200 μm long and 10 μm thick. They usually appear to grade laterally and vertically into secondary shell as the relatively big, irregularly shaped constituents, by which they are distinguished, give way to large then normal-sized, orthodoxly stacked fibres.

Continuous secretion of prismatic calcite gives rise to a layer of closely packed discrete units, up to 20 μm thick and more than 80 μm long, disposed normal to the internal surface. In section they appear as subrectangular bodies each with a convex internal surface representing the surface of accretion at the moment of death (Pl. 24, fig. 4). Sporadically distributed growth bands, up to 400 nm thick, are arranged parallel with these internal surfaces (Pl. 24, fig. 3) and together with traces of acicular crystallites lying normal to the banding, indicate the progress of deposition of the tertiary layer. The rhombic cleavage inherent to each prism is commonly conspicuously developed on the internal surface to define small rhombohedra or crystallites about 20 nm thick (Pl. 24, fig. 1). The cleavage reveals the general non-alignment of adjacent units and emphasizes the latitude used in calling these units 'prisms', because they are more frequently bounded by curved rather than prismatic, dihexagonal or rhombohedral edges.

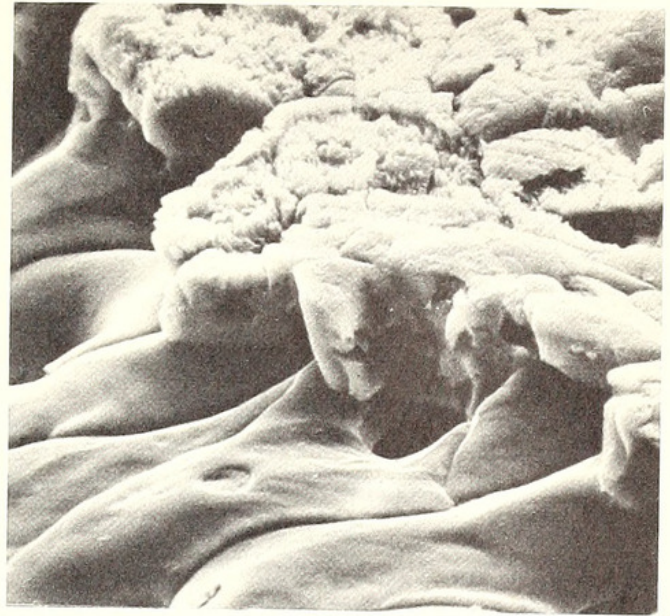
Apart from recording variation in the accretion of the tertiary layer induced by temporal or environmental changes, growth banding also illustrates the relationship between a prism and the fibre from which it arose. Reference has already been made to the highly characteristic attitude of the growth bands seen in the sagittal section of a fibre. Their disposition is, of course, parallel with the profile of the terminal face which is itself determined by the differential rates of accretion of the calcite of the fibre and the protein of its enclosing sheet. The protein sheet exuded by the distal arc of an outer epithelial cell accumulates at about one-twenty-fifth the rate of the calcite deposited by the plasmalemma immediately behind the sheet (Williams 1971, p. 60). Towards the proximal region of the cell, however, carbonate secretion diminishes to a negligible amount. The total effect of such variation in secretory rates is, therefore, the perpetuation of an inwardly bulging terminal face to the fibre accommodated by a complementary concavity in the plasmalemma of the outer epithelial cell, the borders

EXPLANATION OF PLATE 24

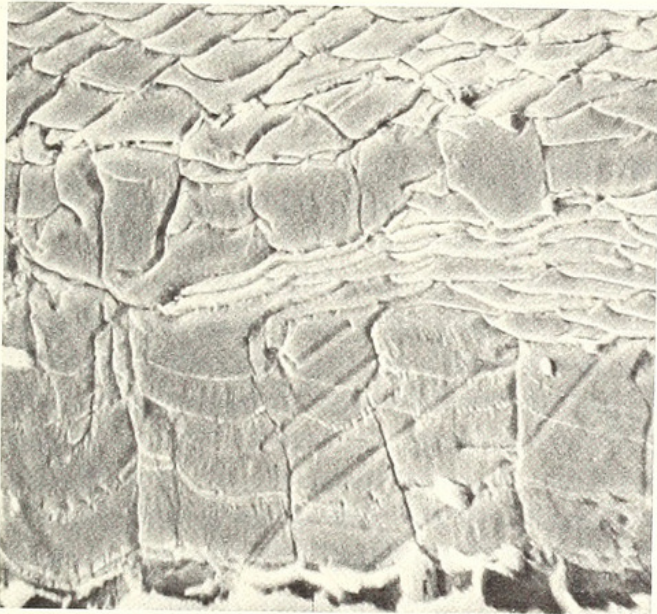
Figs. 1–6. Scanning electron micrographs of the internal surface and sections of a brachial valve of *Liothyrella neozelanica*. 1. Internal surface of the tertiary layer showing the non-alignment of cleavage in adjacent prisms ($\times 2500$). 2. Oblique view of a fractured internal surface of the tertiary layer showing the relationship between prisms and secondary fibres ($\times 1400$). 3–4. Oblique sections showing the relationship between the tertiary layer and an earlier formed lens of prismatic calcite (fig. 3), and secondary fibres (fig. 4) ($\times 1350$, $\times 2600$). 5. Internal surface of the outer zone of the margin of the dorsal adductor scar showing the sporadically developed fibres arising from the prismatic layer ($\times 1300$). 6. Internal surface of the inner zone of the margin of the dorsal adductor scar showing orthodoxly stacked fibres passing into irregular adductor myotest to the left ($\times 1250$).



1



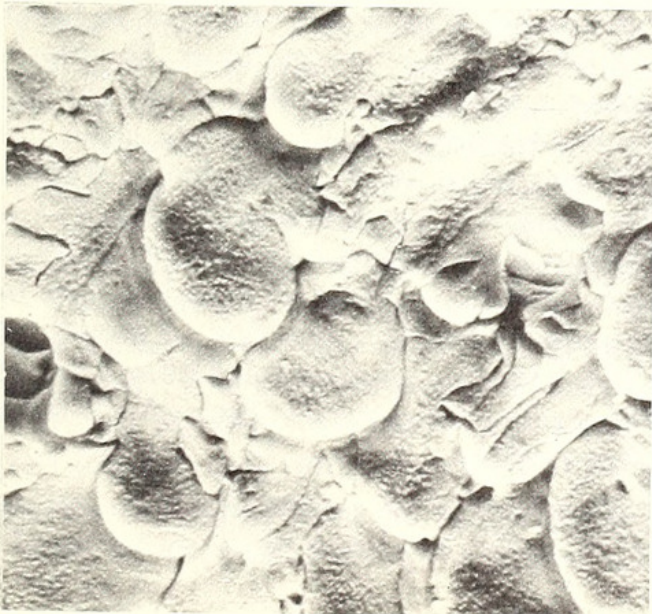
2



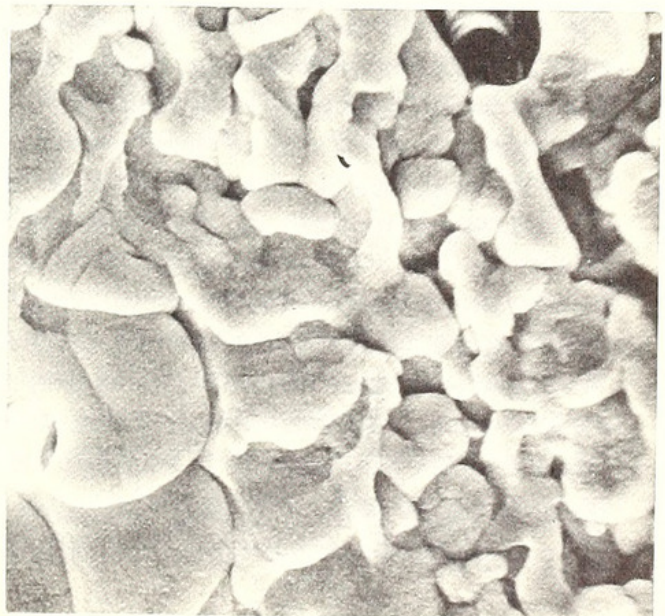
3



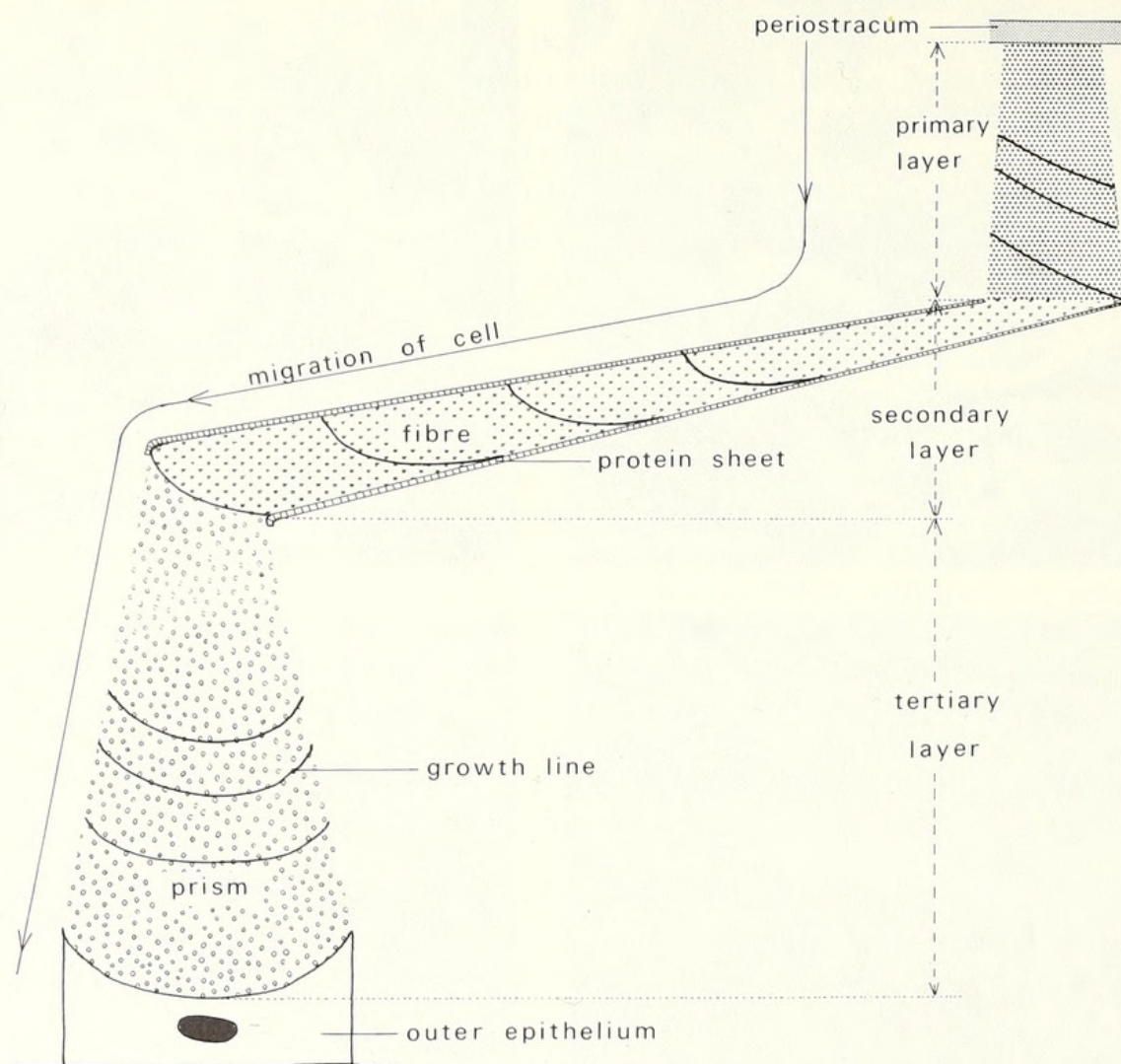
4



5



6



TEXT-FIG. 1. Stylized longitudinal section of part of a valve and mantle of *Liothyrella* showing migration of an outer epithelial cell during its secretion of the mineral shell.

of which are pulled up around the terminal face by desmosomes attached to the investing protein sheets. Two further aspects of the disposition of growth bands in fibres are noteworthy (text-fig. 1). First, the general plane of the terminal faces they represent is inclined at about 30° to the fibres. Secondly, the bands are more or less parallel to those found in the tertiary layer although the general plane of these latter are normal to the long axes of prisms. These different attitudes of growth bands relative to the mineral units of the secondary and tertiary layers are reconcilable if it is assumed that secretion of the carbonate skeleton is essentially normal to the mantle surface, but that secretion of inter-connected proteinous sheets by anterior parts of outer epithelial cells introduces a distal component into the direction of growth of secondary fibres. Cessation of organic secretion, however, removes this bias and causes reversion to the pattern of accretion found governing the growth of the primary layer as is shown by the vertical extension of tertiary prisms.

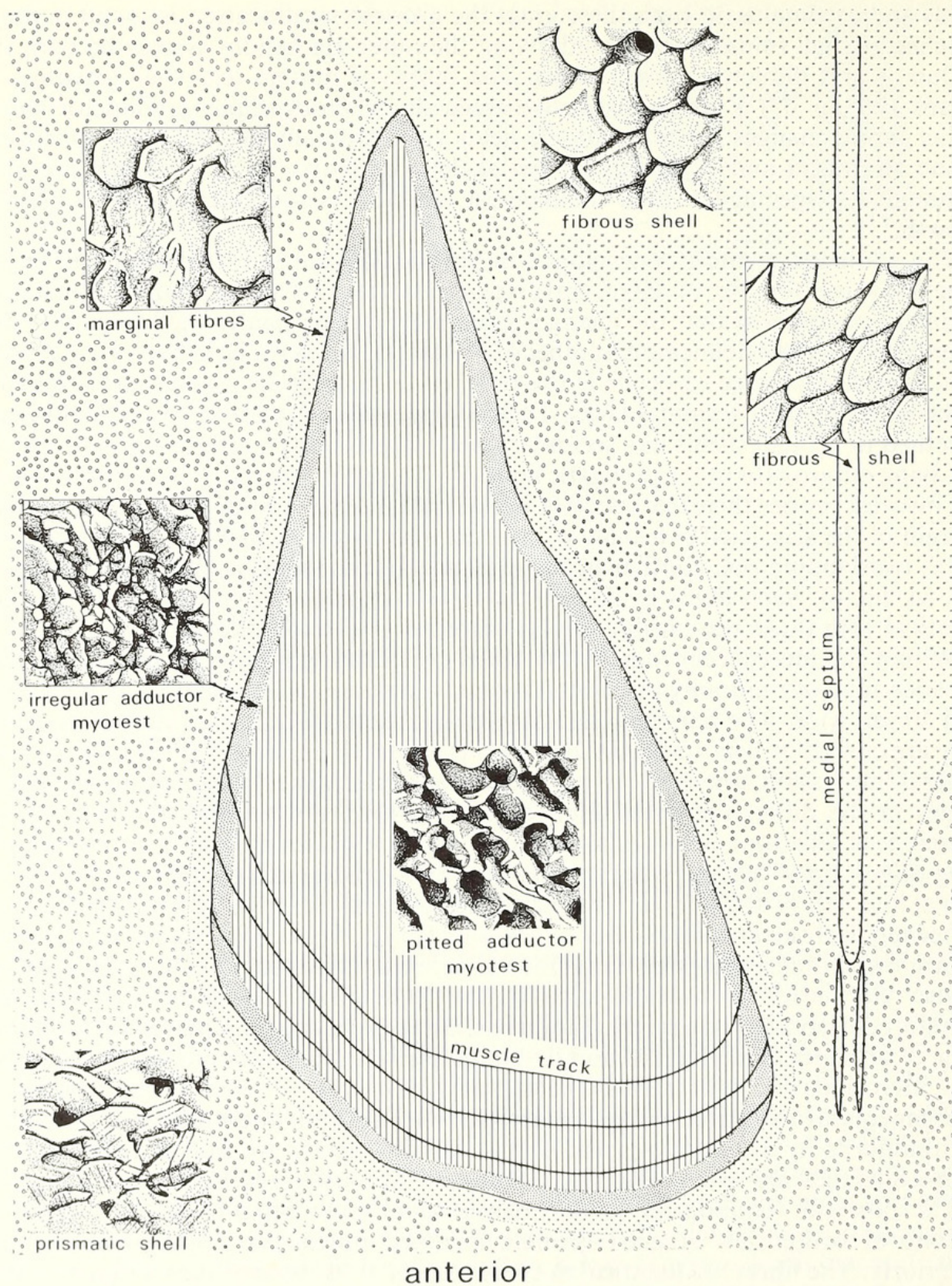
Muscle fields and cardinalia. Tertiary prisms constitute the most widely distributed superficial fabric in the interior of the shell occurring everywhere except in the muscle

fields and cardinalia. In both these areas the grossest modification is found in those patches of shell (muscle scars) underlying the outer epithelium associated with the adductor and diductor muscle bases. The fabric of muscle scar shell (myotest of Krans 1965, p. 65) is highly distinctive especially when overlain by adductor bases. Other fabric changes found in muscle fields and cardinalia are the result of muscle tissue migration and expansion of the skeletal supports for the lophophore and, although less spectacular than the myotest, are no less significant in terms of shell growth.

The adductor myotest is developed in both valves but is better displayed in the brachial valve (text-fig. 2). Here, traverses across the anterior and flanking posterior adductor scars show that the changes from a typical prismatic shell to a fully differentiated myotest delineate a number of concentric zones for each half of the muscle field. The first change to occur is the reappearance of regular fibres with rounded distal edges to their terminal faces. These fibres, which are up to $15\text{ }\mu\text{m}$ across and sheathed in protein sheets like secondary ones, are initially sporadically distributed, flat-lying outgrowths of the prismatic layer (Pl. 24, fig. 5). Inwardly, however, towards the myotest proper their frequency of occurrence increases so that the slightly raised margin of the scar itself is usually coincident with an $80\text{ }\mu\text{m}$ band of closely stacked fibres overlapping one another in the direction of the anterior margin of the valve (Pl. 24, fig. 6). Such fibres could only have been deposited by outer epithelial cells identical with those responsible for the secretion of the secondary layer.

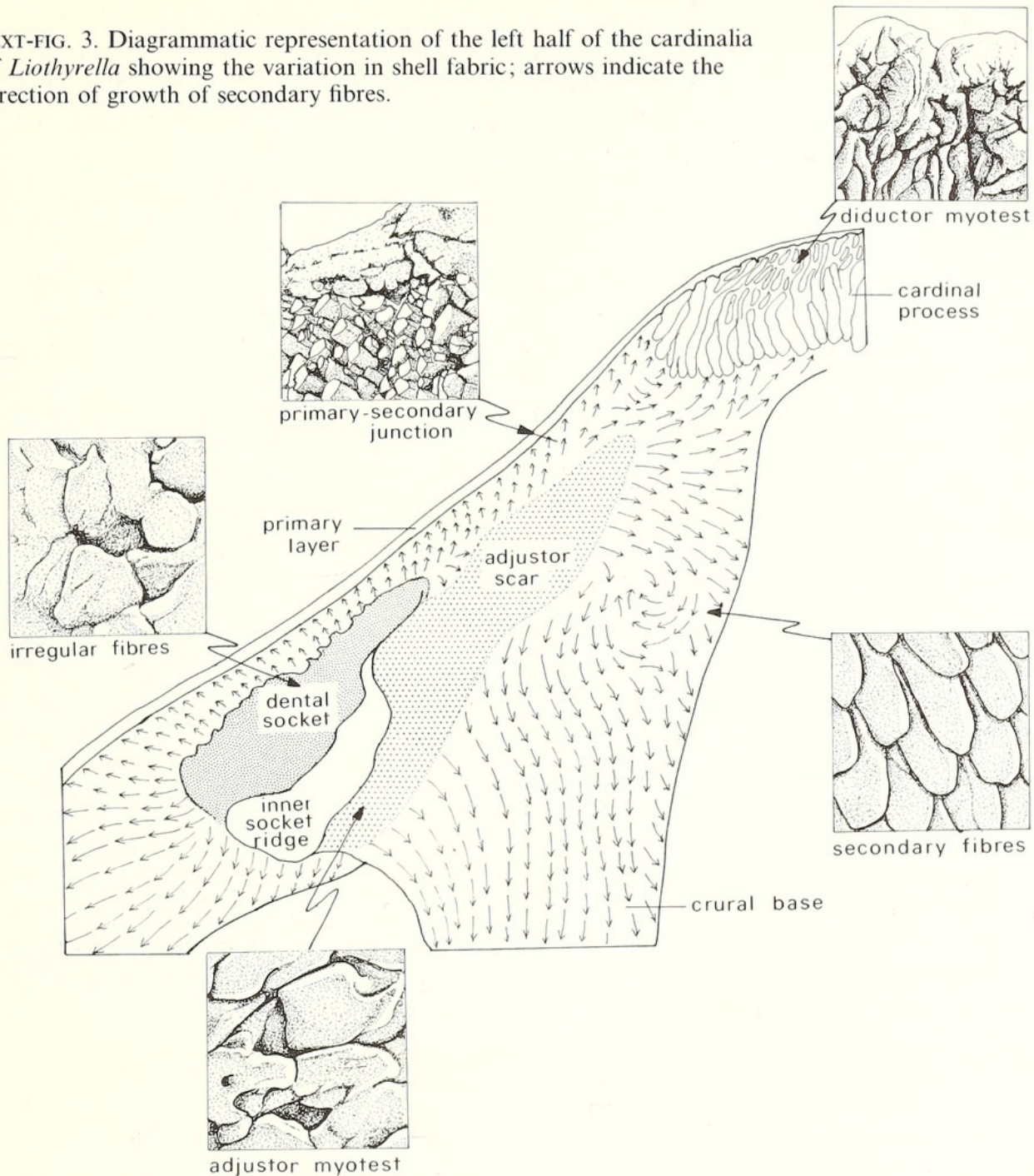
Within the muscle scar margin the fibres are abruptly succeeded by a somewhat broader zone of randomly orientated bars and granules of calcite usually between 5 and $10\text{ }\mu\text{m}$ wide. The bars may be straight and up to $40\text{ }\mu\text{m}$ long; more frequently they are curved or bent to define shallow pits about $10\text{ }\mu\text{m}$ across (Pl. 24, fig. 6). The general impression conveyed by such features is that this zone represents the initial stages in the differential resorption of calcite. Inwardly towards the core of the muscle scar, this zone of irregular adductor myotest passes gradually into a series of long ridges, up to $2.5\text{ }\mu\text{m}$ wide, arranged more or less parallel to the long axis of the scar at intervals of about $5\text{ }\mu\text{m}$. They are linked by cross ridges of the same thickness to define regularly arranged pits about $7\text{ }\mu\text{m}$ long (Pl. 25, fig. 1). The pits are comparable in origin and dimensions with those found in the adductor scars of living *Thecidellina* whose relationship to muscle tissue is known in detail (Williams 1973, p. 456). It is therefore, reasonable to assume that during life each pit accommodates the tonofibril zone of an outer epithelial cell and its bounding ridges correspond to the peripheral and intercellular parts of adjacent cells as in *Thecidellina*. In view of this correlation it seems equally likely that the zone of irregular adductor myotest reflects the presence of tonofibrils in the overlying epithelium although they are not as regularly distributed as they are when cells are associated with muscle bases.

The posterior boundaries of the muscle scars correspond with the margin of a zone of orthodoxly stacked, protein-sheathed fibres overlapping one another anteriorly. The fibres are identical in every respect with those of the secondary shell; but their relative position within the shell succession is significantly different because not only do they transgress forward across the myotest of the muscle scars but also antero-medially across the prismatic shell of the medial septum. The origin of these fibres is best understood in relation to the expansion of the muscle bases.



TEXT-FIG. 2. Diagrammatic representation of the left dorsal adductor scar of *Liothyrella* showing the variation in the fabric of the myotest and the adjoining valve floor.

TEXT-FIG. 3. Diagrammatic representation of the left half of the cardinalia of *Liothyrella* showing the variation in shell fabric; arrows indicate the direction of growth of secondary fibres.



Enlargement of the muscle scars during shell growth results from the antero-lateral migration of the muscle bases away from the umbo as well as an increase in the area of attachment. As the bases expand and shift, an increasing area of outer epithelium first reverts to fibrous secretion and then becomes permeated by tonofibrils. Concomitantly each concentric zone of the muscle scar expands outwards over its neighbour so that those composed of fibres and irregular adductor myotest form two gently inclined layers separating the prismatic shell from a wedge of regularly pitted myotest. Behind the migrating muscle bases, the epithelium reverts to fibrous secretion and the postero-medial areas of all three zones as well as the medial area between the scars are gradually buried by an expanding fibrous layer (text-fig. 2). When first

observed, the occurrence of orthodoxly stacked fibres which are commonly smaller than average, was ascribed to secretion by outer epithelium proliferated in secondary generative zones behind the muscle bases (Williams 1968, p. 16). More recent work, however, has shown that the fibres are secreted by the same cells as deposited myotest at an earlier stage in growth (MacKinnon 1971, p. 38).

In the pedicle valve, traverses across the posterior part of the muscle field show that development of the ventral adductor myotest is accompanied by the same changes as are found in the brachial valve, although on a subdued scale so that adductor pits are not so regularly arranged and are further blurred by closely spaced transverse growth ridges (Pl. 25, fig. 3). The ventral diductor myotest is also differentiated into linearly arranged subrectangular pits, about $7.5\text{ }\mu\text{m}$ across, with prominent transverse growth ridges (Pl. 25, fig. 2). In the brachial valve, however, the dorsal ends of the diductor muscles are inserted in the cardinal process (Pl. 25, fig. 5; text-fig. 3) and are differently accommodated. This ovoid feature situated immediately anterior of the beak consists of forty or more plates diverging on either side of the medial plane. Each plate consists of long intertwined bars, about $5\text{ }\mu\text{m}$ thick, aligned normal to the surface of the cardinal process and culminating in a series of nodules, about $20\text{ }\mu\text{m}$ wide, arranged along the edge of each plate. Resorption pits and slots in the sides of the plates suggest that the muscle bases were inserted not only between plates but also into their sides (Pl. 25, fig. 6).

The fabric of the ventral faces of the inner socket ridges which act as seats of dorsal adjustor muscles is less altered than that of the shell underlying the ventral bases which consists of irregular plates, up to $60\text{ }\mu\text{m}$ across, pitted by resorption. Within the dorsal scars, the secondary fibrous mosaic is modified by the overgrowth of bars and irregular extensions of the terminal faces (Pl. 25, fig. 4). Some resorption pits occur but the fibrous foundation of this myotest layer is still apparent. Indeed irregular granules and bars of calcite, developed on the surfaces of the sockets and the inner side of the loop solely in response to differential growth, form more complex patterns. All these modifications, however, serve to emphasize the prevalence of normally disposed secondary fibres in the cardinalia and the loop and the absence of a tertiary prismatic layer.

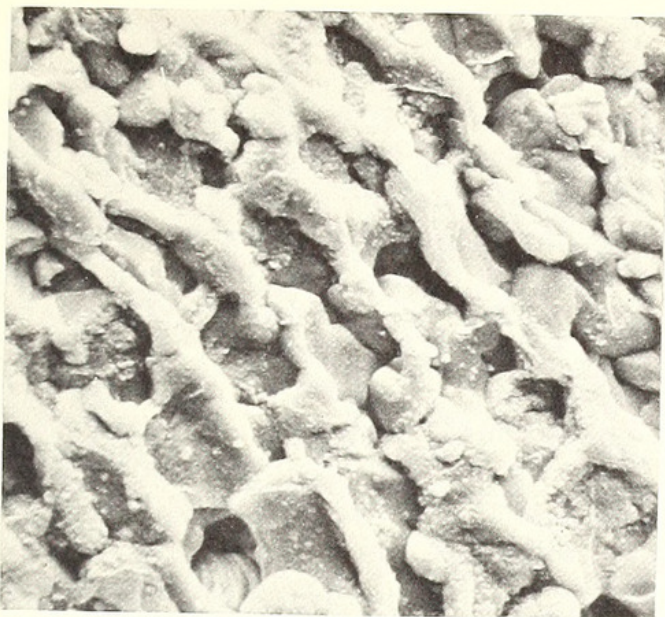
STRUCTURE OF *GRYPHUS* SHELL

Only one other living terebratulid, a mature specimen of *Gryphus vitreus* (Born) from the mid Atlantic south of Portugal, was available for study. The soft parts were too poorly preserved to show the structure of the mantle, but the shell, freed of

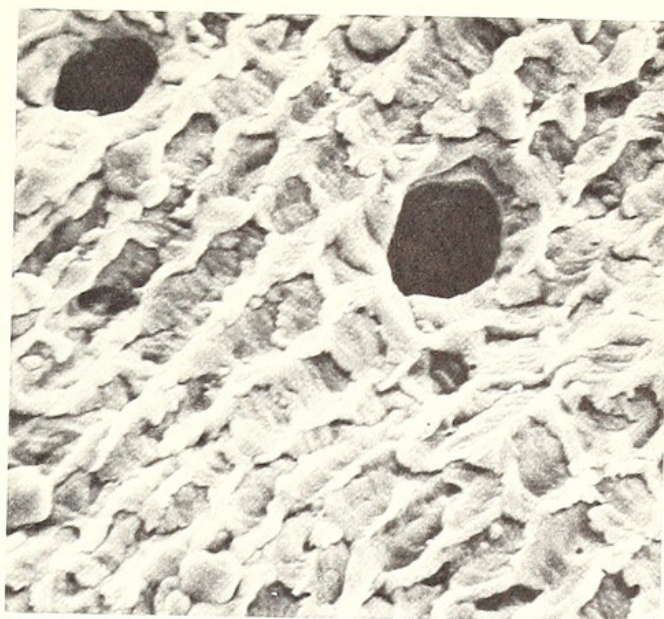
EXPLANATION OF PLATE 25

Figs. 1-6. Scanning electron micrographs of the internal surface of the shell of *Liothyrella neozelanica*.

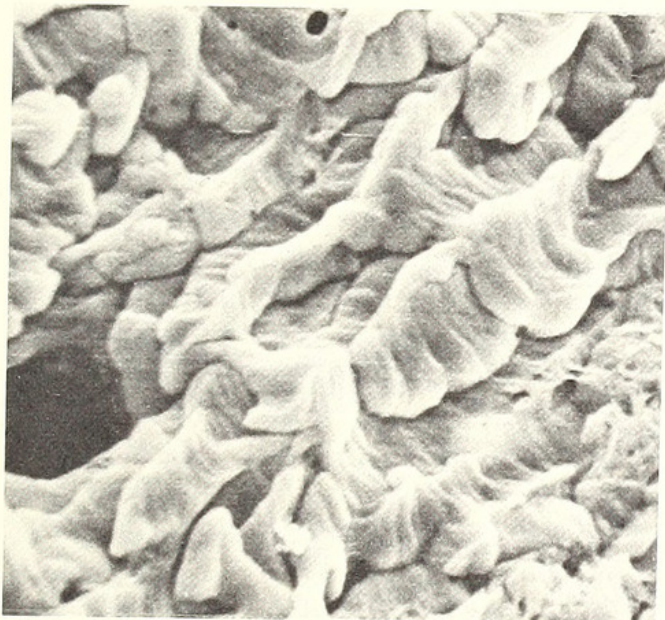
1. Internal surface of the dorsal adductor myotest showing linearly arranged pits ($\times 1300$).
2. Internal surface of the ventral diductor myotest showing the ridges developed in linearly arranged pits ($\times 900$).
3. Internal surface of the ventral adductor myotest showing the less regularly arranged pits ($\times 1900$).
4. Ventral surface of the inner socket ridge showing the dorsal adjustor myotest with irregular growths on the terminal faces of fibres ($\times 1500$).
- 5-6. Ventral views of the cardinal process with details of a plate showing intertwined bars and resorption slots ($\times 75$, $\times 1400$).



1



2



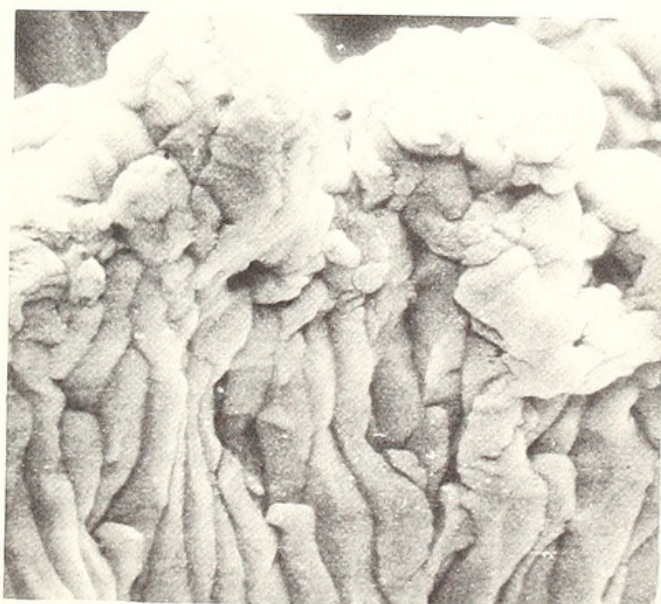
3



4



5



6

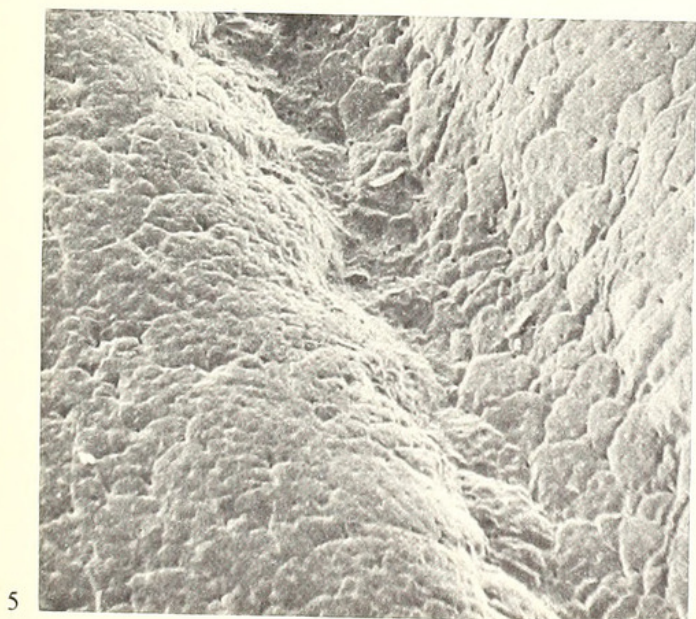
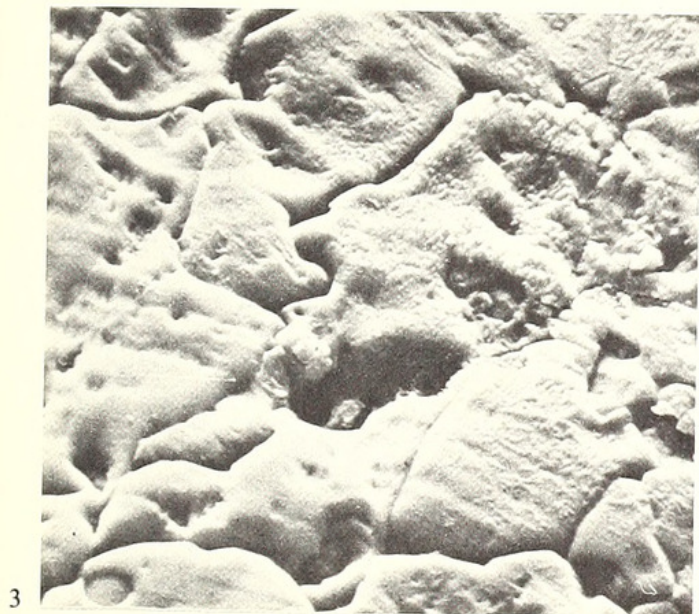
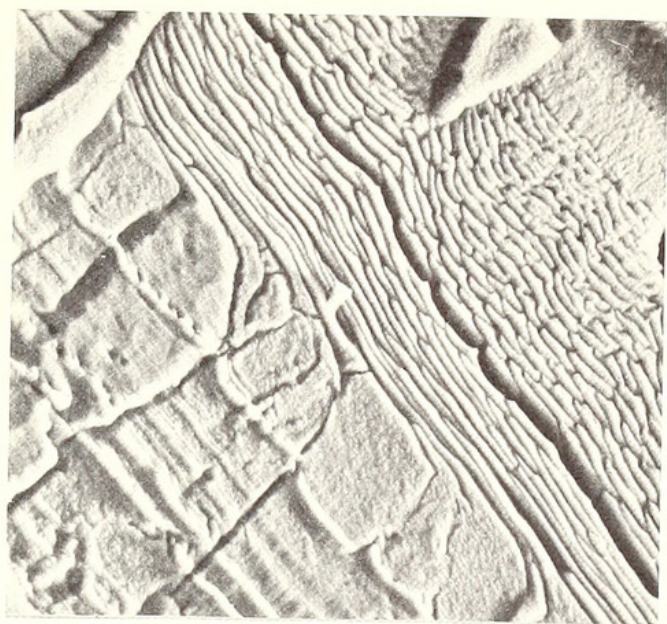
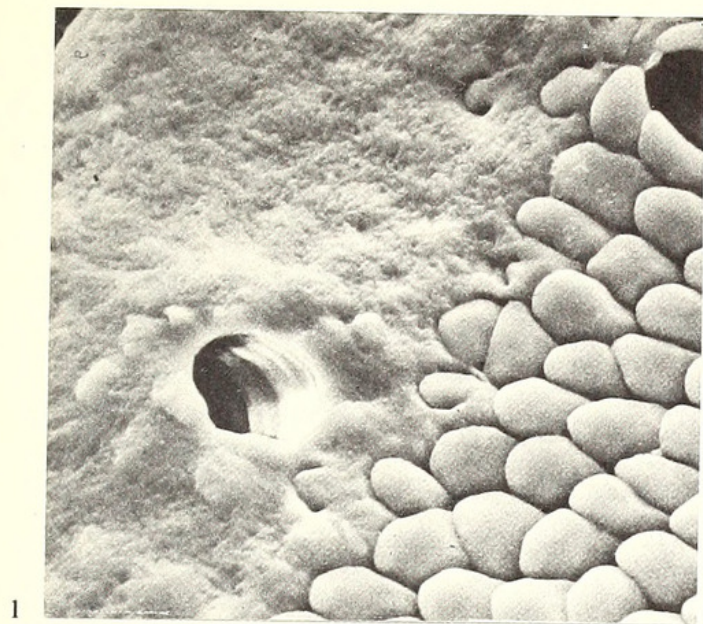
MACKINNON and WILLIAMS, terebratulid shell

adherent tissue, afforded an opportunity to compare the skeletal fabric with that of *Liothyrella* in much greater detail than is possible for fossil species.

The general shell succession is identical with that of *Liothyrella*, differing only in detail and in the relative development of various layers. The primary layer, about 20 μm thick, is mainly composed of acicular crystallites but on a smaller scale than in *Liothyrella* so that the internal surface of the layer at the edge of the valve is much more finely granular (Pl. 26, fig. 1). The first-formed fibres of the secondary layer which is only about 50 μm thick also differ in being almost invariably closely and regularly stacked at low angles to the primary-secondary interface just like mature fibres (Pl. 26, fig. 1). Their transformation into prisms of the tertiary layer, each up to 25 μm thick, is usually conspicuous as is growth banding parallel to the internal surfaces of accretion (Pl. 26, fig. 2). On these surfaces, the prisms again fit together like discrete jigsaw pieces and display angular differences in the dominant cleavage of adjacent units (Pl. 26, fig. 3). Surface features not seen in *Liothyrella* are a series of pits, about 750 nm in diameter, which are fairly regularly distributed at intervals of 10 μm or so in the medial region of the shell. More often than not, the pits appear to be centres of radiating furrows about 700 nm wide (Pl. 26, fig. 4). These furrows are so like macroscopic solution channels that they are tentatively ascribed to differential resorption, while the pits may have been formed by inhibition of carbonate secretion around groups of tonofibrils anchoring the outer epithelium to the inner surface of the tertiary layer. Unlike those of *Liothyrella* or indeed most living brachiopods, the mantle canals are deeply impressed on the internal surfaces of the valves. The *vascula myaria*, for example, are accommodated by a pair of slightly divergent troughs, about 200 μm wide and 150 μm deep (Pl. 26, fig. 5). Such troughs may arise by differential resorption of the shell but in *Gryphus* at least this is not so. The floor and sides of the canal trough are lined with unmodified prismatic calcite (Pl. 26, fig. 6) and must have developed through slower carbonate deposition along that strip of outer epithelium overlying the mantle canal. In contrast to the close similarity in shell succession, the muscle scars of *Gryphus* are quite distinct from those of *Liothyrella*. The adductor myotest was poorly preserved in the specimens examined but it was evident that, although differential secretion and resorption led to the delineation of suboval pits, up to 10 μm across, bounded by calcitic bars, they are irregularly not linearly arranged. The ventral diductor scars are correspondingly less distinctive. Their margins mainly consist of mosaics of calcite plates, up to 30 μm across, usually with

EXPLANATION OF PLATE 26

Figs. 1–6. Scanning electron micrographs of the internal surface and a section of the shell of *Gryphus vitreus* (Born); Recent, mid Atlantic, south of Portugal. 1. Internal surface at the edge of a brachial valve showing both primary and fibrous secondary layers with puncta ($\times 1250$). 2. Section of a mature part of a brachial valve showing the primary layer (top right) and the fibrous secondary layer passing into the prismatic tertiary layer (bottom left); infilled puncta occur in the top left and top right ($\times 650$). 3. Internal surface of the tertiary layer of a brachial valve showing the discrete nature of the prisms ($\times 1300$). 4. Internal surface of the tertiary layer of a pedicle valve showing pits with radiating furrows ($\times 650$). 5. Internal surface of a pedicle valve showing the furrow of a *vasculum myarium* ($\times 120$). 6. Internal surface of a pedicle valve showing the occurrence of typical tertiary prisms in the floor of a *vasculum myarium* ($\times 650$).



MACKINNON and WILLIAMS, terebratulid shell

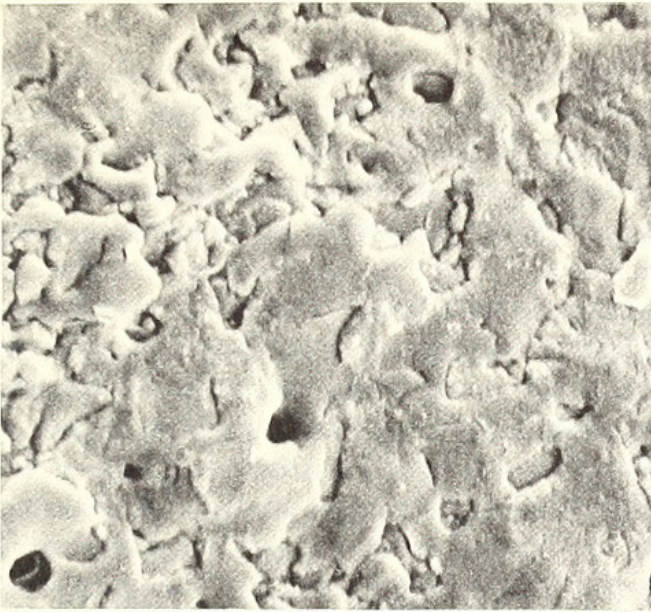
straight boundaries subtending rhombic or prismatic angles. These boundaries become blurred and irregular within the myotest proper while resorption pits are common (Pl. 27, fig. 1). The ventral adjustor myotest is distinguishable from typical prismatic calcite only in the relative absence of surface relief.

STRUCTURE OF FOSSIL TEREBRATULID SHELL

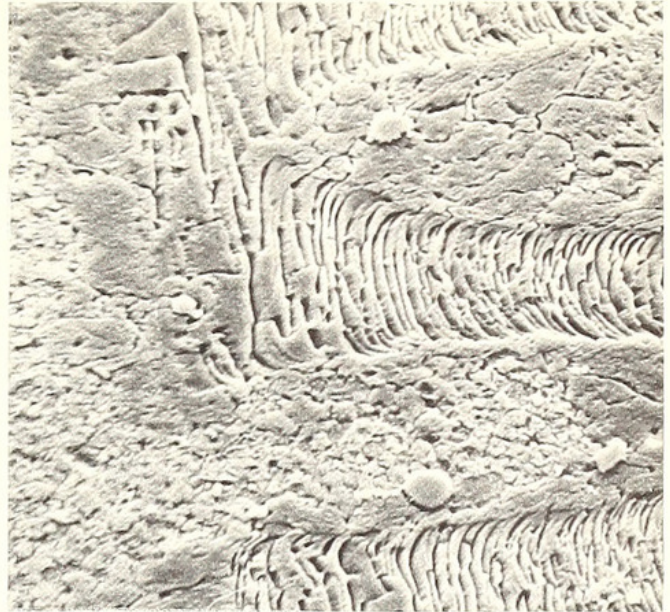
According to Muir-Wood (in Williams *et al.* 1965, pp. H773–800) forty-nine genera, based on wholly extinct species, may be unequivocally assigned to the Terebratulidae. Specimens representing thirty-three of these taxa have been sectioned to determine the shell succession. They are the Jurassic species *Avonothyris plicatina* (Sowerby) (B27389), *Bihenithyris barringtoni* Muir-Wood (B46287), *Cereithyris intermedia* (Sowerby) (B26997), *Charltonithyris uptoni* Buckman (B71348), *Epithyris cf. maxillata* (Sowerby) (B27598), *Euidothyris* sp. (B66893), *Heimia mayeri* (Choffat) (B71369), *Kutchithyris acutiplicata* (Kitchin) (B95464), *Loboidothyris* aff. *latovalis* Buckman (B3706), *Lobothyris punctata* (Sowerby) (B32482), *Lophrothyris etheridgii* (Davidson) (B21808), *Pseudoglossothyris curvifrons* (Davidson) (B52008), *Ptyctothyris stephani* (Davidson) (B13921), *Rugithyris subomalogaster* Buckman (B61079), *Somalithyris macfadyeni* Muir-Wood (B94335), *Sphaeroidothyris globisphaeroidalis* Buckman (B71645), *Stiphrothyris tumida* (Davidson) (B8986), *Stroudithyris pisolithica* Buckman (B28807), *Tubithyris wrighti* (Davidson) (B71258), *Wattonithyris wattonensis* Muir-Wood (B89861), and *Weldonithyris weldonensis* Muir-Wood (B6653); the Cretaceous species *Carneithyris subpentagonalis* Sahni (B51154), *Concinnithyris obesa* (Sowerby) (B7058), *Cyrtothyris cyrta* (Walker) (B21407), *Gibbithyris semiglobosa* (Sowerby) (B5091), *Musculina acuta* (Quenstedt) (B97875), *Neolothyrina obesa* (Davidson) (B51306), *Ornatothyris sulcifera* (Morris) (B24931), ?*Platythyris comptonensis* Middlemiss (B21155), *Praelongithyris praelonga* Middlemiss (B2246), *Rectithyris depressa* (Val), *Rhombothyris extensa* (Meyer) (B25453), and *Sellithyris sella* (Sowerby) (B21931); and the Tertiary species *Terebratula* sp. (B47986). Only in the case of *Bihenithyris* was replacement of the shell so complete as to destroy all traces of the original skeletal fabric. In no species, however, was it possible to determine the nature

EXPLANATION OF PLATE 27

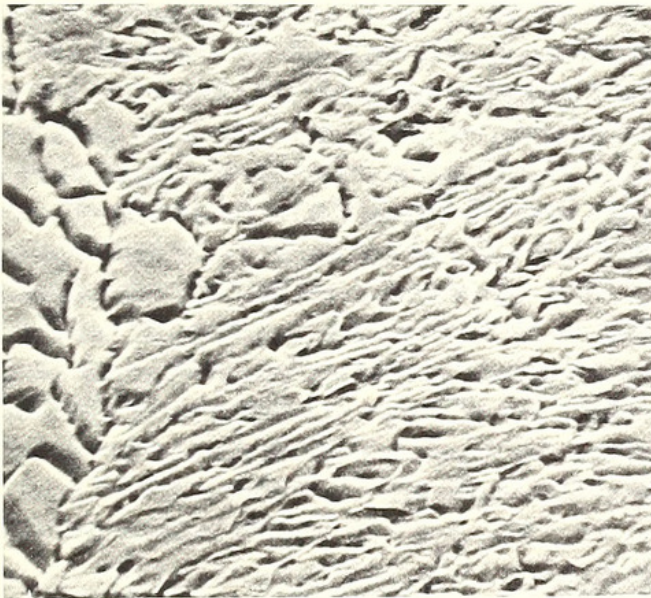
Figs. 1–6. Scanning electron micrographs of various living and fossil terebratulid species. 1. Internal surface of a lateral area of the ventral diductor myotest of *Gryphus vitreus* showing the mosaic of calcitic plates and resorption pits ($\times 1000$). 2. Section showing puncta penetrating a fibrous secondary layer and a relatively thin tertiary layer (to the left) in the shell of *Lophrothyris etheridgii* (Davidson) (B21808), Inferior Oolite, Ravensgate Hill, England ($\times 650$). 3. Section showing acicular and granular crystallites and first-formed fibres of the primary and secondary layers respectively in the shell of *Pseudoglossothyris curvifrons* (Davidson) (B52008), Inferior Oolite, Leckhampton Hill, England ($\times 3000$). 4. Section showing fine-grained sediment (below) filling a punctum in the fibrous secondary succession forming the inner layer in the shell of *Carneithyris subpentagonalis* Sahni (B51154), Senonian, Catton, England ($\times 1400$). 5. Section showing the passage of secondary fibres into tertiary prisms in the shell of *Euidothyris* sp., Inferior Oolite, Misterton, England ($\times 1500$). 6. Section showing the granular tertiary layer, with the junction with the secondary layer above and an infilled punctum to the right in the shell of *Praelongithyris praelonga* Middlemiss (B2246), Lower Greensand, Potton, England ($\times 1500$).



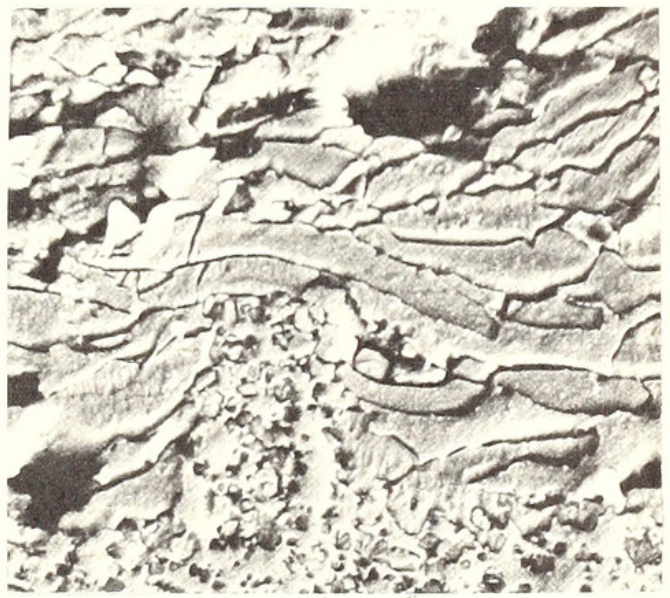
1



2



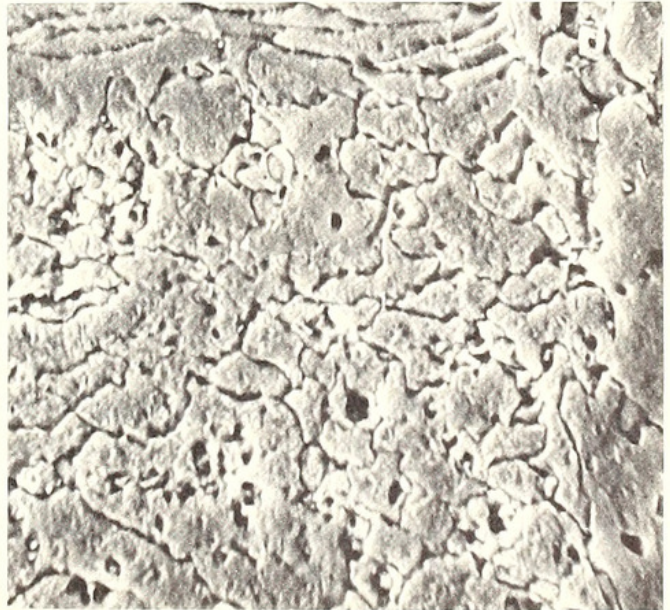
3



4



5



6

of the myotest which consists of thin layers mostly exposed on the floor of the valves and, therefore, subject to gross alteration even by non-penetrative diagenetic processes. Indeed unless techniques are developed to remove the micrite normally covering the surfaces of fossil shells even when free of entombing sediment, the prospects of carrying out a comprehensive survey of the fabric of muscle scars are poor.

Comparison of the shell succession of the species listed above reveals a significant difference only in the relative development of the tertiary layer. All shells are penetrated by regularly distributed unbranched puncta with an average diameter of 10 μm ranging from 6 to 38 μm in *Kutchithyris* and *Tubithyris* respectively. The primary layer is, on average, 53 μm thick varying from 16 μm in *Carneithyris* to 220 μm in *Charltonithyris*. The fabric of most species consists of the same mixture of acicular crystallites and granules, up to 15 and 5 μm in size respectively, as is found in living terebratulids (Pl. 27, fig. 3). In both *Carneithyris* and *Rhombothyris*, however, the texture is predominantly granular. In those species with a tertiary layer, the secondary shell has a mean thickness of 182 μm varying from 46 μm in *Wattonithyris* to 477 μm in *Platythyris*. It consists exclusively of gently inclined, orthodoxly stacked fibres with an average width, when first-formed, of 5 μm ranging from 3 to 8 μm in *Cyrtothyris* and *Concinnithyris* respectively. Identification of the tertiary layer is difficult because its components, even in the unaltered state, may be very like micritic accretions on the inner surfaces of valves which may actually replace parts of the layer and thereby blur its junction with the sediment. The layer, however, like the rest of the shell, is penetrated by puncta and traces of the boundaries within any carbonate underlying a fibrous succession are regarded as indicating the presence of tertiary calcite (Pl. 27, fig. 3). By this means the tertiary layer has been identified in all specimens examined except those assigned to *Carneithyris* (Pl. 27, fig. 4), *Lobothyris*, *Neoliothyris*, *Rhombothyris*, *Terebratula*, and *Tubithyris*. The layer itself may be preceded by thin lenses or even continuous layers (up to 40 μm thick in *Euidothyris*) intercalated with fibres of the secondary shell. It may also contain impersistent lenses of fibres but it consists mainly of large components which, although recrystallized in some species into interlocking rhombohedra, clearly represent the prisms characteristic of the tertiary shell of *Liothyrella* (Pl. 27, fig. 5). The only noteworthy textural variation occurs in *Praelongithyris*, the tertiary layer of which is composed of granules up to 20 μm in size interspersed with irregular fibres (Pl. 27, fig. 6).

CONCLUSIONS

The most interesting aspect of the structure of the terebratulid shell is the stratigraphic and taxonomic distribution of those genera lacking a tertiary layer. The Terebratulidae are usually divided into six subfamilies in the manner proposed by Muir-Wood (in Williams *et al.* 1965, pp. H773–800) although at that time the arrangement of the largest subfamily, the Terebratulinae, was regarded as only provisional (op. cit., p. H773). The family includes the Upper Triassic *Plectoconcha* Cooper, the earliest known terebratulacean, and is generally conceded to be ancestral to the other familial groups assigned to the Terebratulacea with the possible exception of the Orthotomidae. Although the fabric of the *Plectoconcha* shell has not yet been deter-

mined, the fact that another early terebratulid, the Liassic *Lobothyris*, lacks a tertiary layer is consistent with the inferred descent of the terebratulaceans from the dielasmataceans (Stehli 1956, p. 194). The shell structure of species belonging to the latter superfamily has not been systematically investigated but information currently available (Williams 1968, p. 31 and in manuscript) suggests that a succession consisting of only the primary and secondary layers is prevalent. It is, therefore, feasible to infer that the tertiary layer found in the majority of Terebratulidae was acquired gerontomorphically after the emergence of the stock from its dielasmatacean progenitors. Moreover, even when allowance is made for the lack of information about the shell structure of those genera not available for study, the stratigraphic distribution of forms without a tertiary layer is too sporadic and their morphology too disparate to entertain their descent from *Lobothyris* (except for *Tubithyris*) or from one another. Consequently, it is likely that the skeletal succession of the Cretaceous rectithyridinids *Neolothyria* and *Rhombothyris* and the carneithyridinid *Carneithyris*, and even the Tertiary terebratulid *Terebratula*, resulted from a repeated neotenus suppression of prismatic secretion.

With regard to changes in shell fabric resulting from the emplacement of muscle bases, the degree of difference in the myotests of *Liothyrella* and *Gryphus* is unexpected. Studies of the myotests in other living rhynchonellids and terebratulids (Williams 1968; MacKinnon 1971) indicate that the principal modifications include a welding together of secondary fibres and loss of their characteristic outline. Since these changes occur during secretion of the prismatic layer, further modification through muscle attachment should have produced structurally similar myotests. Yet the pits of the adductor myotest of *Liothyrella* are characteristically strongly defined and regularly arranged, while those of the diductor myotest have no counterpart in *Gryphus*. Such differences suggest a deeper, more oblique insertion of the muscle bases into the *Liothyrella* shell. It is, therefore, possible that important factors in determining the fabric of the myotest are the disposition of the muscles relative to the valve floors as well as their strength.

Acknowledgements. We are indebted to Miss Anne Brunt of the Fisheries Research Division (Wellington) of the New Zealand Marine Department and Mr. Ellis Owen of the British Museum (Nat. Hist.) for providing us with living and fossil species. We also wish to thank Dr. Jean Graham, Research Assistant in the Department of Geology, The Queen's University, Belfast, for help in the preparation of illustrations, and the Natural Environment Research Council for grants for the 'Stereoscan' scanning electron microscope and for the post-graduate grant held by MacKinnon from 1968 to 1971.

REFERENCES

- ALEXANDER, F. E. S. 1948. A revision of the genus *Pentamerus*, James Sowerby 1813 and a description of the new species *Gypidula bravonium* from the Aymestry limestone of the main outcrop. *Quart. J. geol. Soc. Lond.* **103**, 143-161.
- AMSDEN, T. W. 1964. Brachial plate structure in the brachiopod family Pentameridae. *Palaeontology*, **7**, 220-239.
- CARPENTER, W. B. 1853. On the intimate structure of the shells of Brachiopoda. In DAVIDSON, T., *British fossil Brachiopoda*, **1**, 23-40. Palaeontograph. Soc. London.
- CLOUD, P. E., Jr. 1942. Terebratuloid Brachiopoda of the Silurian and Devonian. *Spec. Pap. Geol. Soc. Amer.* **38**, 1-182.

- GAURI, K. L. and BOUCOT, A. J. 1968. Shell structure and classification of Pentameracea M'Coy, 1844. *Palaeontographica*, **131**, Abt. A, 79-135.
- KING, W. 1871. On the histology of the test of the class Palliobranchiata. *Trans. Roy. Ir. Acad.* **24**, 439-455.
- KRANS, TH. F. 1965. Études morphologiques de quelques spirifères dévoniens de la Chaîne Cantabrique (Espagne). *Leidse geol. Med.* **33**, 71-148.
- MACKINNON, D. I. 1971. Studies in shell growth in living articulate and spiriferide Brachiopoda. Ph.D. thesis. Queen's Univ., Belfast.
- OWEN, G. and WILLIAMS, A. 1969. The caecum of articulate Brachiopoda. *Proc. Roy. Soc. B.* **172**, 187-201.
- ST. JOSEPH, J. K. S. 1938. The Pentameracea of the Oslo region. *Norsk geol. tidsskr.* **17**, 225-336.
- SASS, D. B. and MUNROE, E. A. 1967. Shell-growth in recent terebratuloid Brachiopoda. *Palaeontology*, **10**, 298-306.
- STEHLI, F. G. 1956. Evolution of the loop and lophophore in terebratuloid brachropods. *Evolution*, **10**, 187-200.
- WILLIAMS, A. 1956. The calcareous shell of the Brachiopoda and its importance to their classification. *Biol. Rev.* **31**, 243-287.
- 1968. Evolution of the shell structure of articulate brachiopods. *Spec. Pap. Palaeont.*, No. 2, 1-55.
- 1971. Comments on the growth of the shell of articulate brachiopods. *Smithson. Contributions to Paleobiology*, **3**, 47-67.
- 1973. The secretion and structural evolution of the shell of thecideidine brachiopods. *Trans. Roy. Soc. B.* **264**, 439-478.
- *et al.* 1965. *Treatise on invertebrate paleontology* (ed. Moore, R. C.): *Part H. Brachiopoda*. 927 pp. Lawrence (Univ. of Kansas).

D. I. MACKINNON

Department of Geology
The University of Canterbury
Christchurch
New Zealand

ALWYN WILLIAMS

Department of Geology
The Queen's University of Belfast
Belfast BT7 1NN
Northern Ireland

Manuscript received 29 January 1973



MacKinnon, David Ironside and Williams, Alwyn. 1974. "Shell structure of Terebratulid brachiopods." *Palaeontology* 17, 179–202.

View This Item Online: <https://www.biodiversitylibrary.org/item/197169>

Permalink: <https://www.biodiversitylibrary.org/partpdf/173236>

Holding Institution

Smithsonian Libraries and Archives

Sponsored by

Biodiversity Heritage Library

Copyright & Reuse

Copyright Status: In Copyright. Digitized with the permission of the rights holder.

License: <http://creativecommons.org/licenses/by-nc/3.0/>

Rights: <https://www.biodiversitylibrary.org/permissions/>

This document was created from content at the **Biodiversity Heritage Library**, the world's largest open access digital library for biodiversity literature and archives. Visit BHL at <https://www.biodiversitylibrary.org>.